DEEP NEURAL NETWORK APPROACH FOR VEHICLE IDENTIFICATION IN INTELLIGENT TRANSPORTATION SYSTEMS

K.M.N.Syed Ali Fathima[1*], Dr.K.Merriliance[2]

[1]Research Scholar, Register No: 18131172282016, Sarah Tucker College (Autonomous), Manonmaniam Sundaranar University, Abishekapatti, Tirunelveli - 627 012, Tamil Nadu, India. syedalifathima639@gmail.com

[2]Associate Professor, Research and Department of computer Application, Sarah Tucker College (Autonomous), Tirunelveli- 627 007, Tamil Nadu, India, merrilliance@gmail.com

ABSTRACT

Accidents can be decreased by detecting and tracking vehicles. Objects in the frame are located, along with their positions and classifications, by vehicles. Regionally based item detection was successful, according to researchers. We suggest a region-based deep learning network to find vehicles. Region-based learning is used by faster and grid-based RCNNs. The suggested method can find multiple automobiles. The primary duty of ITS is vehicle classification. This study suggests categorizing vehicles based on their points of view using an SVM and HOG. Numerous items are examined. The plan can assist law enforcement in both securing the car from thieves and physically identifying it via videotaped surveillance. Despite SVM's accuracy, its execution time is unreasonably long due to human fatigue from watching numerous movies and photos. Employing a business is expensive. CNN categorizes vehicle views using SVM, Decision Tree, Random Forest, etc. Today, the method enhances vehicle viewpoint classification. Front, back, and side perspectives are used in the suggested classification of the vehicle. Images of cars are categorized by CNN. According to the evaluation, DeepVehicleNet can function effectively in practical transportation and autonomous driving systems. ITS applications benefit from vehicle-re-identification. The SCRM Network is suggested in this study to increase the accuracy of vehicle re-identification. The Scale-Integrated Feature Mapping Framework of this network extracts notable channel features. The suggested work performs better than earlier ones.

Keywords: Grid RCNN, DeepVehicleNet, SCRM, CBCL, KITTI, VERI, VRIC

DOI Number: 10.14704/nq.2022.20.13.NQ88263 **Neuro Quantology 2022; 20(13):2102-2114**

1. INTRODUCTION

The field of computer visualization focuses on how computers can enhance future image perception. In order to deliver numerical or symbolic information, computer visualization projects gather, assess, develop, and decide on digital images as well as extract high-dimensional data from the actual world. Vehicle detection is a problem for image processing. It is commonly used in computer vision. Understanding an image necessitates not just classifying various representations but also roughly estimating the locations of various elements inside each representation. The ability to recognize objects, a major problem in computer visualization, can help with interpreting linguistic images. Through careful research, objects were discovered. On road images, deep learning-based vehicle detection performs well. With significant brightness, occlusion, and object level discrepancies, real-time vehicle detection fails. This research recommends region-based deep learning rather than processing the entire image.

Reconnaissance images are widely available in well-known cities. Connecting inspection structures watch while also penetrating. The focus of this study is on actions from many angles. Analysis and ITS used by the probing analyzer for scope. The searching analyzer requires viewpoint information as well as vehicle categorization for vehicle detection. The detector/analyzer frequently watches only verified videos and photos. The analyzer/inertia detector starts to have issues after some time. These issues can be resolved by using transportation organization to enhance the front, back, and side views of the vehicle. There are various methods used to classify vehicles.

Re-ID can identify vehicles from different cameras. The application of this research to traffic flow analysis and surveillance stands out. This study collects data on roads and their surrounds, such as vehicle and person counts, in order to estimate traffic flow, improve transportation design, control traffic signals, and obtain information on roads and their surroundings. These programs will improve automated driving, real-time monitoring, and traffic analysis. Re-id devices frame checking, object recognition, feature extraction, and target feature summary.

2. RELATED WORKS

One of the key issues in computer vision research is vehicle detection. Region-based techniques have accelerated recent improvements in object detection. It has been demonstrated by Basri and Jacobs [1] that separating nearby locality limitations for detection has advantages. According to Edelman et alhypothesis,.'s these puzzling neurons may be capable of coordinating and detecting 3D things from a variety of angles. On the gradient image, PCA was applied by Ke and Sukthankar[3]. The 36-dimensional descriptor produced by the PCA-SIFT utilised in this work is quick for matching. Decreasing false-positive rates compared to the best Haar wavelet-based detector from [2] by a factor of more than an order of magnitude.

A quick R-CNN network was suggested by Girshick et al.[4] that takes a complete image as input. To produce a conv highlight map, the system first processes the entire image with a few convolutional (conv) and max-pooling layers. A location of interest (RoI) pooling layer at that moment eliminates a fixed-length highlight vector from the component map for each article proposal. Each element vector is handled by a collection of fully connected (Fc) layers that eventually split into two kin yield layers: one layer that generates softmax likelihood evaluations over K object classes in addition to a general "foundation" class, and another layer that generates four real esteemed numbers for each of the K object classes. For one of the K classes, each set of 4 attributes encodes a refined jumping box position. Faster R-CNN, an approach for object identification that joins the Region Proposal Network (RPN) as a Region of Interest (RoI) applicant extractor, was proposed by He et al. [5]. A faster R-CNN [5] becomes increasingly active to handle the enormous range of vehicle various scales. The Grid R-CNN [6] object detection and identification framework structure replaces the traditional relapse definition with a lattice point led confinement tool and effectively utilises unambiguous spatial depictions for superb limitation. Grid R-CNN uses a fully convolutional network and isolates the item jumping region to matrices. Using distinct scale convolution parts (1X1, 3X3, and 5X5) and a similar component map in a given layer, GoogleNet[7] is a deep learning structure. By using multi-scale features and combining these highlights into a yield highlight map, this technique is discovered. Five groups of convolutional layers and three FC layers make up the VGG Net [8]. The first two groups each have two convolutional layers, and the following three groups each contain three convolutional layers. A Max Pooling layer is added between each group to reduce the spatial element.

In order to advance recognition, ResNet [9], which reduced optimization complexity by incorporating shortcut relations, extracts attribute embed of the whole reflection and concatenates it with area characteristic. The repressed features from shallow layers were replicated and acquired by DenseNet [10], which retains the deep layer characteristics and performs better in sequence flow by coupling the input with the remaining output. He et al[11] .'s Mask R-CNN proposal called for the creation of bounce boxes and division covers in accordance with the concept, followed by the use of RoIPool or RoIAlign to extract features. Following the use of the extort features for additional proposal degeneration and classification, the ROI Align layer, which addressed the quantization problem by bilinear introduction at partially examined positions inside each grid, is trained using an integrated occurrence segmentation framework, and the detector is optimised with pixel-level supervision. He et al. [11] and Dai et al. [12] are the authors of this work. The multi-stage R-CNNs are successively more prevalent for precise localization thanks to Cascade R-CNN [13], which prepares multi-stage R-CNNs with rising IOU threshold phase-by-phase.

The Faster-RCNN reproduction was combined with two different convolutional neural networks (VGG-16 and ResNet-50) by Ren et al. [14] [15]. Because of the poor concentration accuracy of the preset anchor and single-stage deterioration, RetinaNet [16] focuses on resolving the localization precision of single-stage detectors. RefineDet is a two-step degradation that recovers single-stage detectors using two-step pour ground loss in order to increase concentration precision for single-stage detectors.

Cars can be classified by graphic images obtained from an RGB camera or a gray-level image [17] during the day or at night, but not by vision-based photographs obtained at night if there is sufficient lighting. As a result, more types of information are needed as input to a detector used at night by a vehicle like an automobile. Anchor box clustering is accomplished using the YOLO [18] deep learning runs algorithm and is based on the training set's ground truth. This algorithm then recovers its behaviour for the specific dataset. Using the best feature representation extracted, the shortened classification accuracy challenge following template-based feature extraction is separated. Vehicle classification network using CNN learning and Spatial Pyramid Pooling (SPP) overcomes the issue of accuracy truncation brought on by image resizing-induced image falsification. There are classifications described in two sorts, i.e. different types of cars and variations of the colour, by combining CNN with SVM and normalising features in SVM [19–24]. Minsize, Midsize, Max Size, and Unidentified are the four categories used in classification. Eight classes—black, white, blue, green, yellow, magenta, red, and unexplained hues—are used to categorise colours.

Unidentified variations are included in classifications based on type and colour. Variations of the class include overlay vehicles on colour variations like brown colour, unclear qualities on the vehicle, and unrelated colour variations on the vehicle [18, 25, 26–28]. General potential purpose for the many categories used to categorise the vehicle's type and colour. A classifier uses a Support Vector Machine to train a Histogram Oriented Gradient to extract the feature vector [29-33] of training models for the categorization of vehicles. According to the movement classification on vehicles, the vehicle types of vehicles are divided into major types, such as mini cars, small cars, compact cars, medium cars, medium and large cars, luxury cars, Audi, SUV, Sedan, Benz, etc. The HOG feature vector of samples on test is positioned into the classifier to find the classification result of test samples used by SVM.

In-depth elements-based frameworks have been proposed as a solution to the problems with the hand-crafted elements-based classifiers. CNN-based semi-regulated arrangement technique for consistent vehicle order has been introduced by Dong et al. [34]. The softmax layer has been created to calculate the class likelihood of having a place vehicle, and a sparse Laplacian channel-based technique has been developed to extract relative vehicle data. - The introduced technique achieved 96.1% and 89.6% precision in the constant photos, respectively, when tested on the BitVehicle dataset. Wang et al. [35] have developed a Fast R-CNN based vehicle order technique for traffic reconnaissance in an ongoing environment in another exploration effort. On an intersection dataset of 60,000 images that was collected and divided into preparation and tested data, the intended approach achieved 80.051% accuracy. CNN and a start to finish integrated design have been suggested by Cao et al. [36] for vehicle grouping in the inclement street conditions. The CompCars view-mindful dataset was used to test the proposed system, and the desired classifier achieved a precision rate of 0.953. According to Chauhan et al. [37], the best way to arrange vehicles is to use interstate streets and a CNN-based vehicle order structure. According to creators, the suggested approach successfully completed 75% MAP on the dataset of 5562 CCTV camera recordings of thruway traffic. An exchange learning-based GoogLeNet system for vehicle grouping in street traffic has been foreseen by Jo et al. [38]. The classifier's authors have demonstrated that it successfully analysed the ILSVRC-2012 dataset with a precision rate of 0.983. According to Kim et al. [39], the PCANeT-HOG-HU based combined include extraction approach is what is needed by SVM to create the arrangement model. In addition, for the preparation and testing of the proposed characterization organisation, the creators have gathered the dataset consisting of 13700 images of vehicles representing six vehicle classifications (i.e., cruiser, van, vehicle, truck, smaller than usual transport, and enormous transport). Results showed that on the provided dataset, the proposed lightweight classifier achieved 98.34% normal precision.

For related applications such vehicle re-identification, various CNN models [40] were applied. Examples of applications comparable to vehicle re-identification include image recognition, image detection, and human re-identification [41–43]. Deep learning-based methods [44, 45] indicate greater performance for re-id approaches when compared to methods based on hand-crafted features. The majority of these methods use measures like N-pair loss [47], triplet loss [46], and angulate loss [48] to train using the suitable networks. Some works collect more data, such as colours, poses, and vehicle types [49]. There are numerous further studies that produce fresh images, including domain randomization [50] and generative adversarial networks [51].

3. METHODOLOGY

3.1 DATASET DESCRIPTION

The Street Scenes Challenge Framework is a collection of images, annotations, software and performance measures for object detection. Each image was taken from a DSC-F717 camera at in and around Boston, MA. Each image was then labeled by hand with polygons surrounding each example of 9 object categories, including [cars, pedestrians, bicycles, buildings, trees, skies, roads, sidewalks, and stores]. The labeling of these images was done under scrutiny to ensure that objects were always labeled in the same way, with regard to occlusions and other common image transforms. Street Scenes labels are also compatible with LabelMe annotations, with a one to one conversion tool, provided here. http://cbcl.mit.edu/software-datasets/streetscenes/

Our tasks of interest are: stereo, optical flow, visual odometry, 3D object detection and 3D tracking. For this purpose, we equipped a standard station wagon with two high-resolution color and grayscale video cameras. Accurate ground truth is provided by a Velodyne laser scanner and a GPS localization system. Our datsets are captured by driving around the mid-size city of Karlsruhe, in rural areas and on highways. Up to 15 cars and 30 pedestrians are visible per image. Besides providing all data in raw format, we extract benchmarks for each task. https://www.cvlibs.net/datasets/kitti/

Existing vehicle re-identification (re-id) evaluation benchmarks consider strongly artificial test scenarios by assuming the availability of high quality images and fine-grained appearance at an almost constant image scale, reminiscent to images required for Automatic Number Plate Recognition, e.g. VeRi-776. Such assumptions are often invalid in realistic vehicle re-id scenarios where arbitrarily changing image resolutions (scales) are the norm. This makes the existing vehicle re-id benchmarks limited for testing the true performance of a re-id method. In this work, we introduce a more realistic and challenging vehicle re-id benchmark, called Vehicle Re-Identification in Context (VRIC). In contrast to existing datasets, VRIC is uniquely characterised by vehicle images subject to more realistic and unconstrained variations in resolution (scale), motion blur, illumination, occlusion, and viewpoint. It contains 60,430 images of 5,622 vehicle identities captured by 60 different cameras at heterogeneous road traffic scenes in both day-time and night-time. https://qmul-vric.github.io/

To facilitate the research of vehicle re-identification (Re-Id), we build a large-scale benchmark dateset for vehicle Re-Id in the real-world urban surveillance scenario, named “VeRi”. The featured properties of VeRi include: (https://vehiclereid.github.io/VeRi/)

- It contains over 50,000 images of 776 vehicles captured by 20 cameras covering an 1.0 km^2 area in 24 hours, which makes the dataset scalable enough for vehicle Re-Id and other related research.
- The images are captured in a real-world unconstrained surveillance scene and labeled with varied attributes, e.g. BBoxes, types, colors, and brands. So complicated models can be learnt and evaluated for vehicle Re-Id.

- Each vehicle is captured by 2 ~ 18 cameras in different viewpoints, illuminations, resolutions, and occlusions, which provides high recurrence rate for vehicle Re-Id in practical surveillance environment.
- It is also labeled with sufficient license plates and spatiotemporal information, such as the BBoxes of plates, plate strings, the timestamps of vehicles, and the distances between neighbouring cameras, datasets are depicted in Table.1.

Table.1 – Details about the Dataset

Dataset	Training (85%)			Testing (15%)	Total
KITTI	6137			1083	7220
CBCL	4446			784	5230
VERI – 776	**Image test**	**Image train**	**Query image**		
	11579	37778	1678		
VRIC	**Gallery image**	**Probe images**	**Train images**		
	2811	2811	54,808		

3.2 Vehicle Detection using GRID R-CNN

A lattice directed restriction component is added to Grid R-CNN [52], another object detection system, to help identify objects precisely. Grid R-CNN [52] reframes the localization problem as a classification problem by using explicit spatial representation to estimate the location of the grid points. The first recognition structure that locates the object by predicting network focuses at the pixel level is Grid R-CNN [52]. You can obtain matrix focal points with excellent confinement outcomes. Highlights of return on investment are then applied to carry out arrangement and restriction. We acquire a framework-guided tool for superb restriction, in contrast to earlier efforts with a container balance relapse branch. The likelihood heat map produced by the framework expectation branch, which incorporates an FCN [53], allows us to identify the matrix focuses in the bouncing box aligned with the article. We finally determine the precise item bouncing box using the lattice focuses and a data combination strategy at the element map level. The proposal is initially created for multi-stage identifiers, and then RoIPool or RoIAlign are used to extract highlights from the objects. The Grid RCNN object detector's architecture is provided Fig.1.

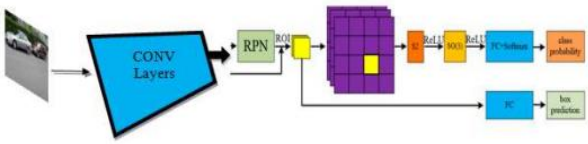

Fig.1 – GRID RCNN Architecture

Grid-CNN with approximately 180 boxes in a multi-scale lattice performs better than Fast R-CNN that makes use of about 2K proposition-based bounding boxes. By eliminating the item proposal stage and reducing the number of boxes that must be handled, this approach speeds up recognition. It also trains a regressor to incrementally shift and scale grid components in the direction of objects. High-quality object localisation is achieved via grid R-CNN. Grid R-CNN combines the conventional relapse-based techniques with a lattice-guided limitation instrument for precise item recognition. Grid R-CNN effectively captures spatial data and enhances the position-sensitive feature of a fully convolutional architecture. Using the CBCL train dataset, do SGD for 30k mini-batch cycles, then reduce the learning rate to 0.0001 and get ready for an additional 10k cycles. After 40,000 cycles, learning comes to an end, and for quicker preparation, the borders of layers conv1-1 through conv2-2 are fixed. Run SGD on the CBCL vehicle dataset for small scale clump emphases, then lower the learning rate and train for various cycles. On loads and dispositions, a force and boundary rot are used.

3.3 Vehicle Viewpoint Classification using SVM-HOG

Local people who are worried about an image rising in the histogram may define the vehicle. Then, a histogram piece's gradient can be found to precisely characterise the grade positioning in small portions of the image on spitting, validating initial entries. Contour extractor is HOG. This method divides the finding window into a number of units that are encompassing the surrounding space, and these units are then over separated into precise points in a huge, thick gridiron above the finding window. These units are further divided into points, and information about slope is mined from the points in order to produce on an image's gradient. Take K (p, q), which provides information merely about the significance of (x, y), and suppose its slope directions.

$$\nabla K(p,q) = \begin{bmatrix} k_p \\ k_q \end{bmatrix} = \begin{bmatrix} \frac{\partial_k}{\partial_p} \\ \frac{\partial_k}{\partial_q} \end{bmatrix} = \begin{bmatrix} k(p+1,q) - k(p-1,q) \\ k(p,q+1) - k(p,q-1) \end{bmatrix} \quad (1)$$

Calculated rate k_p and k_q be located at that point in order to apply this calculation of significant parameters such as inclination degree and ascending angle using a puzzle whose magnitude ranges from 1 to -1 is referred to as an essential variance.

$$g_{deg}(p,q) = \sqrt{k_p(p,q)^2 + k_q(p,q)^2}$$

$$k_{ang}(p,q) = tan^{-1} \frac{k_{q(p,q)}}{k_p(p,q)} \quad (2)$$

The histogram is built using a degree and angular matrix and involves numerous ampoules, where each ampoule displays a certain angle represented [0, 22/7]. A certain pixel on the angle is computed to approximate a specific point in the gradient. Result of a number of gradients pointing in the direction of each point in the frame. The vector used to create the space for the article is the merging of all gradient points. A classifier that is resolved by the individual point is the SVM. SVM's ideal value is determined via

$$sgn(w^T Ø(x) + b) = sgn(\textstyle\sum_{i=1}^{l} y_i \propto_i K(x_i, \quad (3)$$

Where w is the solution vector, represents the label, I represents the weights of the vector, and K (xi, x) represents the kernel function. As a result of the effective structure of the Support Vector Machine, the parameter y_i I b, names are labels, support vectors, and parameter of kernels is saved.

3.4 Viewpoint–Based Feature Extraction using Proposed DeepVehicleNet

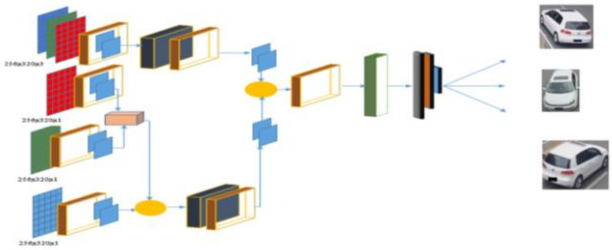

Fig.2 - Proposed DeepVehicleNet

Every channel transmits information differently. The channel that has the most information available can be used for feature extraction if we can locate it. A channel mask will be used to produce channel responses. Three interconnected series of operations are applied to the input image, and then they are concatenated using a layer. That concatenated output is fed into the convolution layer, which feeds into the flatten layer, which feeds into the dense layer, which is used to classify viewpoints. The four unique series of processes each employ a convolution filter with a size of 5 X 5, 3 X 3, 3X3, and 3X3. The input x RGB includes three channel input in the first series is fed into a convolution 2D layer with 64 5 X 5 filters, which perform batch normalisation and RELU with a maximum pooling size of 2 X 2, and whose output is fed into a convolution 2D layer with 118 3 X 3 filters, which perform batch normalisation and RELU with a maximum pooling size of 2 X 2. Up until the bottom right corner of the input image is reached, this process is repeated. Although a truncation is performed separately for each element in the input by an activation layer using the RELU function, the input size is not altered. This activation function increases the nonlinearity of the CNN.

Fourth series (B) whose output is concatenated that output fed into convolution 2D layer having sixty-four 3X3 filters, which performs batch normalisation with a maximum pooling of 2 X 2 size, and second (R) and third series (G) whose output is concatenated that output fed into average pooling layer, The input x B channel is fed into the fourth series together with the output from the first and second series fed into the convolution 2D layer containing sixty-four 3 X 3 filters. This layer does batch normalisation, activation layer (RELU) with max pooling of 2 X 2, and it has sixty-four 5X5 filters.

The input,x R channel is fed into a convolution 2D layer with 64 5X5 filters in the second series, which performs batch normalisation, RELU with a maximum pooling of 2 X 2 size. In the third series, a convolution 2D layer with 64 5X5 filters that performs batch normalisation and an activation layer (RELU) with a maximum pooling of 2 X 2 size is fed the input,x G channel. That concatenated output is fed into the dense layer, whose output is fed into the Softmax for classification, which is a convolutional 2D layer with 64 3X3 filters that performs batch normalisation and activation with flattening and dense layers of 512 size that have been reduced to dense layers of 256 size.

3.5 Vehicle Re-Identification

The height-wise partition for a vehicle can be used to accomplish re-identification, however due to the difficulty of the process, it is not recommended for Re-ID. Through the improvement of the visual perception system, this work seeks to enhance the representation of global features. Many researchers utilise the Re-ID approach to concentrate on the objective rather than the backdrop. The portions of an image that have the greatest meaning to the user are the ones that receive the channel's attention. Even if there are more and more works that merge the two categories into one model, most of them still don't model visual attention well enough. In this article, we suggest a technique that will enable us to identify distinguishing elements in photos of vehicles without having an adverse effect on the background. The process is intended to be reliable and effective. The two-stream model of the visual cortex is simulated using a three-branched adaptive attention network. To support the empirical network architecture, it was built (Fig.3).

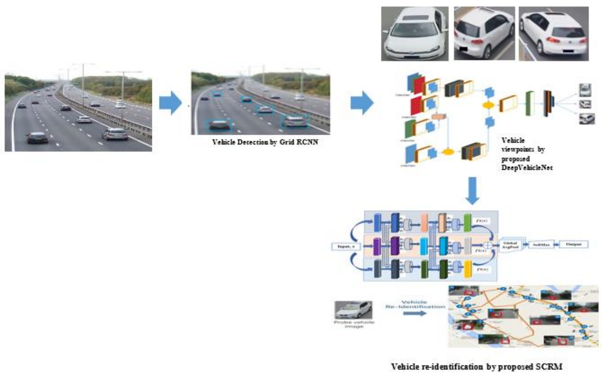

Fig.3 – Vehicle Re-Identification System

3.5.1 PROPOSED SCRM

Fig.4 shows the architecture of SCRM. Thus, the query of re-identifying targeted image can be defined by its descriptor P, and it is formulated as:

$$T = arg_{T_i} \min D\,(T_i Q), T_i \in \mathfrak{I} \qquad (4)$$

Where $\mathcal{T}$ = {T1… TN} is a gallery set of N image descriptors, and D (,) represents the distance metric. Therefore, to solve above the re-id problem, it is important first to answer how can represent targeted object using a descriptor to robust performance.

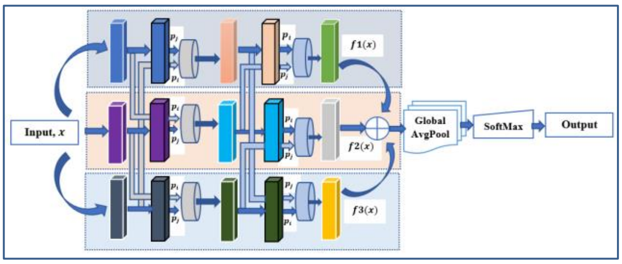

Fig.4 - Vehicle re-identification using proposed SCRM (scale integrated Multi-series residual network)

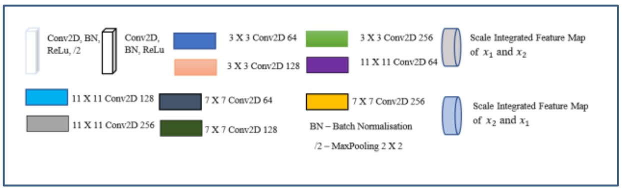

Every channel transmits information differently. The channel that has the most information available can be used for feature extraction if we can locate it. A channel mask will be used to produce channel responses. Three interconnected series of operations are applied to the input image, and then they are concatenated using a layer. This output is concatenated and supplied into a layer called global average pooling, whose output is then fed into a layer called Softmax for classification. The three unique convolution filters used in the three series of operations are 3 X 3, 11 X 11, and 7 X 7, respectively. The input x is fed into a convolution 2D layer with 64 3 X 3 filters in the first series, which performs batch normalisation with a maximum pooling of 2 X 2 size. In a convolution layer, an overlapped convolution kernel is placed on top of the input image. This allows us to calculate the product of the input and the numbers at the same point in the kernel, and then sum these products to obtain a single number. The next convolution result will be generated when the kernel has been pushed down by one pixel. As a result, the convolution kernel is lowered till it touches the input matrix's bottom edge (image). One element will bring the kernel back to the top and to the right (pixel). Up until the bottom right corner of the input image is reached, this process is repeated. Although a truncation is performed separately for each element in the input by an activation layer using the RELU function, the input size is not altered. This activation function increases the nonlinearity of the CNN.

After performing scale integrated feature mapping, the output of the first block in the first series of operations is fed into a second convolution 2D layer with 64 3 X 3 filters with batch normalisation (SIFM). The output from the first block of the third series of operations serves as another input (p i) for this scale integrated mapping. The SIFM's architecture is shown in Figure 6.4. SIFM block accepts p i and p j as inputs. The activation layer with a RELU-based activation function receives the output of the global average pooling layer once the p i has been supplied into it. The dense layer, whose output feeds into another activation layer with a sigmoid function, receives the output of this RELU layer. To obtain the SIFM output, the output of this is reshaped and multiplied by p j. The third block of the first set of operations receives the output of this SIFM.

A convolution 2D layer with 128 3 X 3 filters makes up the third block of the first series and performs batch normalisation with a maximum pooling of 2 X 2 size. A convolution 2D layer with 128 3 X 3 filters makes up the fourth block in this sequence, which receives the output of the third block and performs batch normalisation. Another SIFM block receives the output of this block as its next input, which comes from the output of the third block of the second series of operations. This result is sent into the fifth block of the first series of operations, which is a second convolutional 2D layer with 256 3 X 3 filters and performs batch normalisation with a maximum pooling size of 2 X 2, producing the output f1 (x).

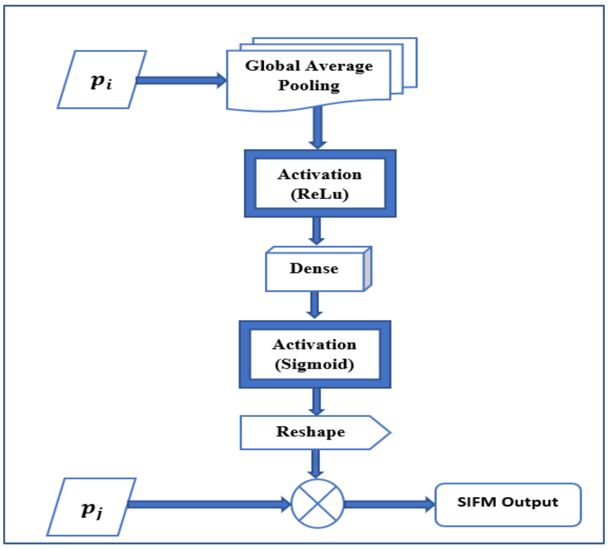

The input,x is fed into a convolution 2D layer with 64 11 X 11 filters in the second series, which performs batch normalisation with a maximum pooling of 2 X 2 size. After performing SIFM, the output of this block is passed into the second convolution 2D layer, which has 64 11 X 11 filters and batch normalisation. The result from the first block of the first series of operations serves as another input for this SIFM. The third block of the second set of operations receives the output of this SIFM. The second series' third block is a convolution 2D layer with 128 11 X 11 filters that performs batch normalisation with a maximum pooling size of 2 X 2. A convolution 2D layer with 128 11 X 11 filters makes up the fourth block in this series, which receives the output of the third block and performs batch normalisation. Another SIFM block receives the output of this block as its next input, which comes from the output of the third block of the third series of operations. This output is sent into the fifth block of the second series of operations, a second convolution 2D layer with 256 11 X 11 filters that performs batch normalisation with a maximum pooling size of 2 X 2, giving the output f2 (x).

In the third series, the input x is fed into a convolution layer with a 2D structure that has 64 7 X 7 filters and performs batch normalisation with a maximum pooling size of 2 X 2. After performing SIFM, the output of this is fed into another convolution 2D layer with 64 7 X 7 batch-normalized filters, whose output is fed into the following block. The result from the first block of the second series of operations serves as another input for this SIFM. The third block of the third set of operations receives the output of this SIFM. The second series' third block is a convolution 2D layer with 118 7 X 7 filters that performs batch normalisation with a maximum pooling size of 2 X 2. A convolution 2D layer with 128 7 X 7 filters makes up the fourth block in this sequence, which receives the output of the third block and performs batch normalisation. This block's output is fed into another SIFM block, whose subsequent input comes from the third block of the first set of operations' output. This output is passed into the fifth block of the third series of operations, a second convolution 2D layer with 256 7 X 7 filters that performs batch normalisation with a maximum pooling size of 2 X 2, giving the output f3 (x). Concatenated and fed into the global average pooling layer, whose output is classified using the Softmax layer, are the intermediate outputs f1(x), f2(x), and f3(x).

4. RESULT AND DISCUSSION

This part evaluates our enhanced vehicle detection technique, which was created by fusing faster and grid RCNN. The average precision (AP), confusion matrix, precision, recall, and IoU are used to do this. Because the CBCL object identification benchmark uses the display of the vehicle classification as the assessment average, rate the performance of the vehicle class. There are 1000 images total in the CBCL dataset, 85% of which are utilised as training images and 15% as test images.. Dataset Link: http://cbcl.mit.edu/software-datasets/streetscenes/

In the training phase, car photos are chosen as positive models while traffic background images are chosen as negative models to demonstrate the effectiveness of this technique for classifying vehicles from their points of view. SVM was used to train the positive and negative models. More than 3,000 car photos were obtained for the testing dataset. The collection contains a variety of vehicle viewpoint photos, including front, rear, and side views. Vehicle testing experimental stage identification.

It has different input and a different purpose than conventional classification jobs. When it comes to perspective tasks for categorization, DeepVehicleNEts stay completely realistic. The purpose of experiments is to establish the ideal conformation and to identify a fair division of vehicle views. Adam is used to train all networks [35]. The first convolution layer is completed in the starting location, followed by conv., Batch Normalization, and Rectified Linear Units. Weights are initialised and regularisation is used to avoid overfitting. The automobiles in the database will be divided into the front, back, and rear categories. 12450 vehicle viewpoint photos in all are collected in preset classes and carefully labelled. Table I lists the number of each sort of vehicle viewpoint in various iterations. Every experiment is performed using Matlab R2019a on an Intel(R) Core(TM) i5-9300H CPU running at 2.40GHz, a 4790K CPU, and 8GB of RAM. The operating system is Windows 10 64-bit, and training took 5 hours to complete.

By building three parallel stages of ResNets with various convolution kernel sizes, the proposed vehicle re-identification system is designed to retrieve multi-scale data from the inputs. The residuals from various stages are utilised in a crossover fashion to extract finite features. By utilising residuals from various stages, a novel scale-integrated feature mapping approach incorporates channel-wise attention of the input into the structure. The VeRi - 776 performance analysis reveals 94.25% Rank-1 accuracy, while the VRIC performance analysis shows 48.83% Rank-1 accuracy. These results are significantly better than the performance of the existing algorithms.

4.1 Performance Metrics

(i) Perplexity Matrix

The object detection task is utilized to make predicts about item classifications and the directions of existing items. For a solitary ground-truth object, make "valid/invalid" expectation to mean whether ready to prevail with regards to distinguishing the item detecting the object.

(ii) Accuracy

Accuracy gauges how precise your expectations are, demonstrating the level of right positive calculates which is given in Eqn. (5).

$$\text{Precision} = \frac{\text{TA}}{\text{TA+FA}} \tag{5}$$

(iii) Recall

The review quantifies how great our indicator is at discovering all the positives, demonstrating the level of the positive ground-truth protests that locator (faster RCNN and Grid RCNN) finds which is given in Eqn. (6)

$$\text{Recall} = \frac{\text{TA}}{\text{TA+FP}} \tag{6}$$

(iv) Intersection over Union (IoU)

The Intersection over Union (IoU) is an assessment metric in the article location territory. It gauges the covering rate between two zones, which is to quantify how great our locator is as for the ground-truth which is given in Eqn. (7).

$$\text{IoU} = \text{Areaof}\frac{\text{Overlap}}{\text{union}} \tag{7}$$

(v) Standard accuracy

Standard Accuracy is a significant level assessment metric in object discovery, which comprises of an accuracy, review, and IoU. For each ground-truth object, we use our identifier to make expectations and afterwards judge the right forecasts by contrasting IoU and the IoU limit. We at that point process the disarray network, exactness, and review. Then, we likewise utilize a certainty score to quantify how much certainty we have in our identifier. We set the scored edge from 0 to 1 and step size to 0.05, and afterwards, we process the accuracy and review sets which are given in Eqn. (8).

$$AP = \int_0^1 p(r)dr \tag{8}$$

Table -2 - ANALYSIS FOR BASED ON THE PERFORMANCE METRICS

VEHICLE DETECTION BY GRID RCNN					
Dataset	**Accuracy**	**Precision**	**Recall**	**F1-Score**	**mAP**
KITTI	91.88	92.68	93.42	93.04	93.64
CBCL	**92.67**	**94.56**	**94.72**	94.6399	95.12
VERI-776	93.92	95.87	95.65	95.7599	94.38
VRIC	**95.28**	**97.54**	**96.43**	96.9768	96.47
VEHICLE VIEWPOINT CLASSIFICATION BY PROPOSED DEEPVEHICLENET					
KITTI	94.49	94.24	93.75	93.99436	92.13
CBCL	93.7	92.24	93.05	92.64323	93.45
VERI-776	97.69	95.13	94.38	94.7535	94.28
VRIC	94.42	93.43	94.26	93.84316	94.52
VEHICLE RE-IDENTIFICATION BY SCRM					
	rank -1	**rank -5**		**mAP**	
KITTI	90.89	94.87		72.24	
CBCL	90.12	92.14		68.37	
VERI-776	90.36	94.25		78.26	
VRIC	89.64	93.71		67.29	

5. CONCLUSION

Intelligence in sensing, communicating, analysing, and regulating ground transportation enhances smart transportation system efficiency, mobility, and security. The Grid RCNN-trained end-to-end identification of vehicle (car) images performs better. Our technique resolves and improves this field by exchanging flexibility characteristics with an SVM with HOG during training and testing. HOG-based SVM for vehicle image feature extraction. then designated the amount of separate class nearly equivalent to per capita added in individual piece consequently that our network also learns viewpoint class characteristics, our dataset included training images, and the rest of the images were allocated for evaluating the network and trying to test our model on a large number of images so that our real achieved accuracy would be clear, achieved 95.28% of accuracy, 97.54% of precision, 96.43% of sensitivity, and 96.97% of F1-score and 96.47 of mAP in Grid RCNN for vehicle detection, DeepVehicleNet, viewpoint classification method achieved 94.42% of accuracy, 93.43% of precision, 94.26% of recall, 93.84% of F1-score and mAP of 94.52%. Our trained DeepVehicleNet model should help ITS. And confidence that in the imminent, superior benchmark of datasets on vehicles beginning direction or position of the vehicle become supplied, also by consuming them, DeepVehicleNet accuracy increases enhance. After preliminary results, discard that the DeepVehicleNet is real to transportation on classifications the vehicle then stout near their vehicle perspectives. Scale-Integrated Cross Residual Multi-Series (SCRM) Network is proposed to improve vehicle re-identification accuracy. SCRM accomplished 89.64% of rank-1, 93.71 of rank – 5 accuracy and 67.29% of mAP, A Scale-Integrated Feature Mapping Framework adds an attention mechanism for channel features better than the other models.

REFERENCES

[1] Basri, R., and Jacobs, D.W. 1997, "Recognition using region correspondences", International Journal of Computer Vision, 25(2):145-166.

[2] Ke, Y., Sukthankar, R.: PCA-SIFT: A more distinctive representation for local image descriptors. In: CVPR (2). (2004) 506 – 513.

[3] A. Mohan, C. Papageorgiou, and T. Poggio,"Example-based object detection in images by components. *PAMI*, 23(4):349–361, April 2001.

[4] R. Girshick. Fast R-CNN.arxiv:1504.08083, 2015.

[5] Shaoqingren, Kaiming He, Ross Girshick, and Jian Sun. "Faster R-CNN: Towards real-time object detection with region proposal networks." In Advances in Neural information processing Systems, pp. 91-99, 2015.

[6] X. Lu, B. Li, Y. Yue, Q. Li, J. Yan, Grid r-CNN, in CVPR, 2019.

[7] C. Szegedy, W. Liu, Y. Jia, P. Sermanet, S. Reed, D. Anguelov, D. Erhan, V. Vanhoucke, A. Rabinovich, Going deeper with convolutions, in CVPR, 2015.

[8] Karen Simonyan and Andrew Zisserman. "Very Deep Convolutional Networks for Large- Scale Image Recognition." *Computing Research Repository (corr),* abs/1409.1556, 2014.

[9] Kaiming He, Xiangyu Zhang, shaoqingren and Jian Sun. "Deep Residual Learning for Image Recognition."IEEE Conference on Computer Vision and Pattern Recognition(CVPR), 2016: 770-778.

[10] G. Huang, Z. Liu, L. Van Der Maaten, K. Q. Weinberger, Densely connected convolutional networks., in CVPR, 2017.

[11] K. He, G. Gkioxari, P. Dollár, and R. Girshick, "Mask R-CNN", 2017, ICCV , pp. 2980-2988.

[12] J. Dai, K. He, J. Sun, Instance-aware semantic segmentation via multi-task network cascades, in CVPR, 2016.

[13] Z.Cai and N. Vasconcelos, "Cascade R-CNN: Delving Into High-Quality Object Detection", 2018.

[14] Ren Y, Zhu CR, Xiao SP, "Small Object Detection in Optical Remote Sensing Image via Modified Faster R-CNN." Journal Citation Reports., vol.8, no.5, 2018.

[15] Huang Zhongjie, Fu Meixia, Ni Kaili, et al. "Recognition of vehicle-logo based on faster RCNN," 4th International Conference on Signal and Information Processing, Networking and Computers. Vol.494, pp.75-83,2019.

[16] T. Lin, P. Goyal, R. Girshick, K. He, and P. Doll A R, "Focal loss for dense object detection," arxiv preprint ar X iv:1708.02002, 2017.[49] S. Zhang, L. Wen, X. Bian, Z. Lei, and S. Z. Li, "Single-Shot Refinement Neural Network for Object Detection",2018.

[17] Hui-Zhen Gu, Li-Wu Tsai, and Suh-Yin Lee,"Vehicle Size Classification for Real-Time Intelligent Transportation System IEEE International Conference on Intelligent Computing and Integrated Systems (ICISS), DOI: 10.1109/ANTHOLOGY.2013.6784866.

[18] Yunyoung Nam and Yun-Cheol Nam," Vehicle classification based on images from visible light and thermal cameras" DOI 10.1186/s13640-018-0245-2, EURASIP Journal on Image and Video Processing volume 2018, Article number: 5 (2018).

[19] T. Malisiewicz, A. Gupta, and A. A. Efros., "The Ensemble of exemplar svms for object detection and beyond". In ICCV, 2011.

[20] A. Krizhevsky, I. Sutskever, G. E. Hinton, "imagenet Classification with Deep Convolutional Neural Networks." In

Advances in Neural Information processing systems, 2012, pp. 1097–1105.

[21] T.N. Hossein, T. Akihiro, M. Seiichi, M. David, "On-road Multi Vehicles Tracking Using Deformable Object Model and Particle Filter with Improved Likelihood Estimation," IEEE Transactions on Intelligent Transportation Systems, vol.13, pp. 748 - 758, June 2012.

[22] E.A. Zanaty, "Support Vector Machines (svms) versus Multilayer Perception (MLP) in data classification," Egyptian Informatics Journal, Vol. 13, pp. 177-183, November 2012.

[23] L. J. Yang, J. Z. Liu, and X. Tang, "Object detection and viewpoint estimation with the auto-masking neural network," in European Conference on Computer Vision, vol. 8691, pp. 441–455, 2014.

[24] Y. Lecun, Y. Bengio, and G. Hinton, "Deep learning," Nature, vol. 521, no. 7553, p. 436, 2015.

[25] K. Saripan and C. Nuthong, "Tree-based vehicle classification system," 2017 14th International Conference on Electrical Engineering/Electronics, Computer, Telecommunications and Information Technology (ECTI-CON), Phuket, 2017, pp. 439-442.

[26] S.Bougharriou; F. Hamdaoui; A. Mtibaa, "Linear SVM classifier based HOG car detection", ISSN: 2573-539X, DOI: 10.1109/STA.2017.8314922, IEEE.

[27] Penghua Ge, Yanping Hu,"Vehicle Type Classification based on Improved HOG_SVM", 3rd International Conference on Mechatronics Engineering and Information Technology (ICMEIT 2019).

[28] Jinkun Yang, Zhong Chen, Jiahao Zhang, "HOG and SVM algorithm based on vehicle model recognition", Proceedings Volume 11430, MIPPR 2019: Pattern Recognition and Computer Vision; 114300T (2020) https://doi.org/10.1117/12.2538191.

[29] Hui-Zhen Gu, Li-Wu Tsai, and Suh-Yin Lee,"Vehicle Size Classification for Real-Time Intelligent Transportation System IEEE International Conference on Intelligent Computing and Integrated Systems (ICISS), DOI: 10.1109/ANTHOLOGY.2013.6784866.

[30] Yunyoung Nam and Yun-Cheol Nam," Vehicle classification based on images from visible light and thermal cameras" DOI 10.1186/s13640-018-0245-2, EURASIP Journal on Image and Video Processing volume 2018, Article number: 5 (2018).

[31] Stephen Karungaru, Lyu Dongyang, and Kenji Terada,"Vehicle Detection and Type Classification Based on CNN-SVM", IJMLC2021Vol.11 (4):304-310ISSN:2010-3700, DOI: 10.18178/ijmlc.2021.11.4.1052.

[32] K. Saripan and C. Nuthong, "Tree-based vehicle classification system," 2017 14th International Conference on Electrical Engineering/Electronics, Computer, Telecommunications and Information Technology (ECTI-CON), Phuket, 2017, pp. 439-442.

[33] Watcharin Maungmai, Chaiwat Nuthong,"Vehicle Classification with Deep Learning", 2019th IEEE 4th International Conference on Computer and Communication Systems, 294-298.

[34] Liu, X., Liu, W., Mei, T., & Ma. H. (2016). A deep learning based approach to progressive vehicle re-identification for urban surveillance. *European Conference on Computer Vision*, 869–884. Https://link.springer.com/chapter/10.1007/978-3-319-46475-6_53

[35] Mou, L., Xie, H., Mao, S., Zhao, P. & Chen, Y. (2020). Vision-based vehicle behaviour analysis: a structured learning approach via convolutional neural networks. *IET Intelligent Transport Systems*.

[36] Feng, J., Wu, Y., & Zhang. Y. (2018). Lane detection base on deep learning. *11th International Symposium on Computational Intelligence and Design (ISCID)*, pp. 315–318. Https://ieeexplore.ieee.org/document/8695497

[37] Vu T. H., Boonaert, J., Ambellouis, S. & Ahmed, A. T. (2020). Vehicles tracking by combining convolutional neural network based segmentation and optical flow estimation. *International Conference on Advanced Concepts for Intelligent Vision Systems*, pp. 529–540.

[38] Xinchen W., Weiwei Z., Xuncheng W., Lingyun X., Yubin Qian & Zhi Fang. (2019). Real Time Image Processing Real-time vehicle type classification with deep convolutional neural networks. Volume 16, pages 5–14.

[39] Sujatha D Badiger, Dr. M uttarakumari. (2019). Vehicle Classification Using Machine

Learning Algorithms Based on the Vehicular Acoustic Signature. Science, Technology and Development, ISSN: 0950-0707, Volume.8 (11). 369-374. Http://journalstd.com/gallery/38-nov2019.pdf

[40] Kaiming He, Xiangyu Zhang, Shaoqing Ren, and Jian Sun. Deep residual learning for image recognition. In Proceedings of the IEEE conference on computer vision and pattern recognition, pages 770–778, 2016.

[41] Yifan Sun, Liang Zheng, Yi Yang, Qi Tian, and Shengjin Wang. Beyond part models: Person retrieval with refined part pooling (and a strong convolutional baseline). In Proceedings of the European Conference on Computer Vision (ECCV), pages 480–496, 2018.

[42] Guanshuo Wang, Yufeng Yuan, Xiong Chen, Jiwei Li, and Xi Zhou. Learning discriminative features with multiple granularities for person re-identification. In Proceedings of the 26th ACM international conference on Multimedia, pages 274–282, 2018

[43] F. Zheng, C. Deng, X. Sun, X. Jiang, X. Guo, Z. Yu, F. Huang, and R. Ji. Pyramidal person re-identification via multi-loss dynamic training. In 2019 IEEE/CVF Conference on Computer Vision and Pattern Recognition (CVPR), pages 8506–8514, 2019

[44] Haiyun Guo, Chaoyang Zhao, Zhiwei Liu, Jinqiao Wang, and Hanqing Lu. Learning coarse-to-fine structured feature embedding for vehicle re-identification. In AAAI, 2018.

[45] Y Zhou, L Shao, and A Dhabi. Viewpoint-aware attentive multi-view inference for vehicle re-identification. In CVPR, 2018

[46] Alexander Hermans, Lucas Beyer, and Bastian Leibe. In defense of the triplet loss for person re-identification. Arxiv:1703.07737, 2017.

[47] Yifan Sun, Liang Zheng, Weijian Deng, and Shengjin Wang. Svdnet for pedestrian retrieval. In ICCV, 2017.

[48] Jiankang Deng, Jia Guo, Niannan Xue, and Stefanos Zafeiriou. Arcface: Additive angular margin loss for deep face recognition. In CVPR, 2019.

[49] Zheng Tang, Milind Naphade, Stan Birchfield, Jonathan Tremblay, William Hodge, Ratnesh Kumar, Shuo Wang, and Xiaodong Yang. Pamtri: Pose-aware multi-task learning for vehicle re-identification using highly randomized synthetic data. In ICCV, 2019.

[50] Josh Tobin, Rachel Fong, Alex Ray, Jonas Schneider, Wojciech Zaremba, and Pieter Abbeel. Domain randomization for transferring deep neural networks from simulation to the real world. In 2017 IEEE/RSJ international conference on intelligent robots and systems (IROS), pages 23–30, 2017

[51] Zhedong Zheng, Xiaodong Yang, Zhiding Yu, Liang Zheng, Yi Yang, and Jan Kautz. Joint discriminative and generative learning for person re-identification. In CVPR, 2019.

[52] X. Lu, B. Li, Y. Yue, Q. Li, J. Yan, Grid r-CNN, in CVPR, 2019.

[53] J. Long, E. Shelhamer, and T. Darrell.Fully convolutional networks for semantic segmentation.In CVPR, 2015.